Excess heat capacity in a molecular glass: an assessment based on calorimetric and neutron scattering data

1992 J. Phys.: Condens. Matter 4 9581

(http://iopscience.iop.org/0953-8984/4/48/013)

J. Phys.: Condens. Matter 4 (1992) 9581–9594. Printed in the UK

Excess heat capacity in a molecular glass: an assessment based on calorimetric and neutron scattering data

M García-Hernández†, R Burriel‡, F J Bermejo†, C Piqué‡ and J L Martínez§||

† Instituto de Estructura de la Materia, Consejo Superior de Investigaciones Científicas, Serrano 123, E-28006 Madrid, Spain

‡ Instituto de Ciencia de Materiales de Aragón, Consejo Superior de Investigaciones Científicas—Universidad de Zaragoza, Ciudad Universitaria, E-50009 Zaragoza, Spain

§ Institut Laue–Langevin, 156X, F-38042 Grenoble Cédex, France

Received 27 July 1992

Abstract. The constant-pressure heat capacity C_p for an organic glass (methanol) as well as for its polycrystalline reference state, have been measured by adiabatic calorimetry. The data are then analysed using estimates for the constant-volume contribution obtained from results of lattice dynamics calculations (for the polycrystal) and molecular dynamics calculations (for the glass). The temperature variation of C_p is then compared with that derived from the frequency distributions measured by incoherent inelastic neutron scattering. The excess of vibrational modes which appear in the glassy state and become more pronounced at temperatures below 10 K is finally discussed and its origin is tentatively assigned.

1. Introduction

The anomalous thermal properties of glasses at temperatures well below the thermodynamic glass-transition T_g still remain to be understood on a quantitative basis. In recent times, most of the known phenomenology which dominates below 1 K has been successfully accounted for within the framework of the two-level-states (TLS) formalism in terms of tunnelling motions of some (yet to be specified) atoms [1]. In relatively simple systems, such as the orientational glasses formed by alkali-halide–alkali-cyanide mixtures, a truly quantitative interpretation of thermal (specific heats) and transport properties at intermediate temperatures is at present emerging [2]. However, the corresponding properties of topologically disordered solids still constitute a challenge for any attempt to account for their origin, which can be considered to be as universal as most of the properties of the glassy state [3].

A previous study [4] was devoted to the analysis of the low-frequency dynamics of a molecular glass-former (methanol CH_3OH) by means of incoherent inelastic neutron scattering (INS), as well as molecular dynamics (MD) calculations performed for the glassy state alongside lattice dynamics (LD) computations for the polycrystalline reference state. The glass which is formed by quenching the liquid at moderate

|| Permanent address: Departamento de Física Aplicada C-IV, Facultad de Ciencias, Universidad Autónoma de Madrid, E-28049, Madrid, Spain.

0953-8984/92/489581+14$07.50

cooling rates is substantially more complicated, due to the presence of the hydrogen-bond network, than the current van der Waals glasses formed by complex organics or polymers. Nevertheless it was chosen since the small size of the molecular unit enables the comparison of the experimental results with MD calculations performed using a sufficiently large number of particles.

The constant-volume heat C_v capacities calculated from the computer results were found in the previous study to lie substantially below those determined from the vibrational densities of states obtained from the INS experiments, and one of the aims of the present work is to clarify the origins of such a discrepancy. On the other hand, the present work will try to assess the reliability of the generalized frequency distributions (or $g(E)$ vibrational densities of states) obtained from the INS experiments by means of a comparison of the molar heat capacity calculated using such distributions with that determined by calorimetric means. For such a purpose, experimental measurements of the constant-pressure heat capacities C_p have been carried out, which will enable the quantitative evaluation of the different components contributing to the total value.

The outline of the paper is as follows: section 2 comprises the information regarding the experimental measurements; section 3 is devoted to the presentation of the main results and approximations; and finally a discussion of the present results as well as a comparison with those previously obtained are given in section 4.

2. Experimental details

The sample was prepared using commercially available methanol and adding distilled water up to a concentration of six per cent molar in order to stabilize the glassy phase.

The high-resolution measurements were carried out using the IN6 time-of-flight (TOF) spectrometer located on one of the cold neutron guides at the Institut Laue–Langevin (ILL), Grenoble, France. The MD computations were performed by means of temperature quenches of a simulation box containing 256 particles corresponding to the equilibrated liquid at $T = 300$ K [5], with continuous rescaling of the particle velocities. Two glass configurations were analysed corresponding to $T = 35$ K and $T = 10$ K after equilibration lasting 110 ps. The absence of crystallinity was assessed by means of computation of the static $S(Q)$ structure factors, and the reader is referred to the previous work for details concerning the measurements data analysis as well as the molecular and lattice dynamics computations.

Heat capacity measurements were performed using an adiabatic calorimeter. The sample container was a 1 cm^3 vessel fitted with an electrical heater and a Minco platinum resistance thermometer. A few kPa of helium inside the vessel enables rapid thermal equilibration of the sample. A computer controlled data adquisition system was used throughout the measurements, and the adiabaticity was controlled by means of differential thermocouples installed between the sample container and different parts of the adiabatic shields which were interfaced through the instrument program with a digital temperature controller. The molar heat capacity was obtained after subtraction of the contribution from the empty vessel which was measured in a separate run.

The quench into the glassy state was achieved by rapid cooling of the liquid at a rate of about 0.2 K s^{-1}, whereas the polycrystal was formed by slow cooling of about

10 K per day. The absence of any crystalline contamination of the glass was assessed by monitoring the complete disappearence of the glass-transition singularity.

3. Results

The total heat capacity for a molecular material may be written, after taking into consideration the contributions of the internal degrees of freedom, as

$$C_v^{tot}(T) = C_v^{intra}(T) + C_v^{inter}(T) = C_v^{harm} + \Delta C_v^{anh} \tag{1}$$

$$C_p^{tot}(T) = C_v^{tot}(T) + \frac{\alpha^2 V T}{\chi_s(T)} \tag{2}$$

$$C_p^{tot}(T) - C_v^{tot}(T) = C_p^{inter}(T) - C_v^{inter}(T) \tag{3}$$

where the superscripts intra and inter indicate the contributions to these magnitudes arising from internal (molecular modes) and external (intermolecular) degrees of freedom, α and χ_s denote the expansion coefficient and isothermal compressibility and V is the molar volume, C_v^{tot} comprises both harmonic and anharmonic contributions, and the last equation is simply given in terms of the expansivity contribution since the internal modes contribute to C_p and C_v to the same extent.

The C_v^{intra} contribution can be calculated to a reasonable precision by standard statistical thermodynamics on the basis of the decoupling of internal molecular modes from those of lattice origin, once the molecular vibrational frequencies and geometry are known and assuming there is no strong overlap between internal and external modes.

For such an electrical insulator at the temperatures and frequency ranges of interest, the electronic contributions may be disregarded and, therefore, only the internal molecular vibrations contribute significantly to the intramolecular part of the heat capacity. The lowest-lying internal modes correspond to rotations of the methyl group (torsional motions) and the stretching of the C–O bond, as well as couplings between these modes. This contribution can be evaluated easily, once the molecular geometry (moments of inertia), and the set of lowest-lying vibrational frequencies are known, from [6, 7]

$$C_v^{intra}(T) = R\left(\sum_i^f \frac{x_i^2 e^{x_i}}{(e^{x_i} - 1)^2} + Z''_{tors}/Z_{tors} - (Z'_{tors}/Z_{tors})^2\right) \tag{4}$$

$$Z_{tors} = \sum_l^\infty \exp[-(E_l - E_0)/k_B T] \tag{5}$$

$$Z'_{tors} = \sum_l^\infty \exp[-(E_l - E_0)/k_B T][(E_l - E_0)/k_B T]$$

$$Z''_{tors} = \sum_l^\infty \exp[-(E_l - E_0)/k_B T][(E_l - E_0)/k_B T]^2$$

$$E_l = (l + \tfrac{1}{2})\hbar\omega_{tors}$$

$$\omega_{tors} = 3\sqrt{V_0/2I_r} \tag{6}$$

where R stands for the gas constant, the first summation runs over the four [8] combination modes due to the coupling of the C–O stretch with torsion and bendings, $x_i = E_i/k_B T$, and Z_{tors} denotes the partition function for the internal methyl torsional modes. Two quantities are required for the calculation of the latter magnitude from the E_l internal rotational energy levels, which are the height V_0 of the potential barrier (this was taken from [9] to be 48.3 meV) and the moment of inertia of the methyl group (which was evaluated to be 5.232×10^{-47} Kg m^2). Although the internal high-frequency C–O stretching vibration does not give any significant contribution to the heat capacity (the value of this quantity for $T = 100$ K gives about 10^{-2} J K^{-1} mol^{-1}), the torsional contribution provides about one fourth of the total C_v at the same temperature.

In order to estimate the intermolecular contributions (which include the translation and rotation of molecules) the $C_v^{inter}(T)$ function was evaluated from the frequency distributions calculated by means of LD computations for the polycrystal and MD simulations for the glass. The MD simulations were performed using an interaction potential which treats the molecule as a rigid unit and has been validated previously for the study of dynamical properties of the cold liquid, crystal and glass phases [5, 4]. The contributions to the heat capacity from the internal modes are then added to those of intermolecular origin since, as mentioned before, all the internal contributions appear at frequencies above 20 meV (232 K), thus being well separated from the low-frequency part of the excitation spectra of both polycrystal and glass phases.

The difference between constant-pressure and constant-volume heat capacities is customarily given as

$$C_p^{total}(T) - C_v^{harm}(T) = \alpha^2 VT/\chi(T) + \Delta C_v^{anh}(T) \tag{7}$$

where the last term in the summation comprises all these anharmonic effects of intermolecular origin.

In order to estimate the contribution due to thermal expansion effects, the molar volume data were taken from a recent constant-pressure MD simulation on glassy methanol [10], and the compressibility was estimated from reported values for the sound velocity and density [4, 5]. The thermal expansion coefficient was calculated from the simulation data [10] since $\alpha = (1/3V)(\partial V/\partial T)_p$. Such a contributions has been found to be less than 1 J K^{-1} mol^{-1} at the highest explored temperatures (around 100 K).

The heat capacity values were also calculated from the generalized frequency distributions $g(E)$ derived from the INS experiments according to the usual expression for molecular materials

$$C_v^{tot}(T) = 6R \int_0^{E_{max}} \frac{x^2 e^x}{(e^x - 1)^2} g(E)\, dE \tag{8}$$

where $x = E/k_B T$. The upper limit of the integration was taken as 40 meV, and at the lowest temperatures (5 K and 10 K), corresponding to the INS measurements, an extrapolation of $g(E)$ in E^2 was used in order to remove the contamination arising from the tails of the broadened elastic line (resolution effects) for energy transfers below 0.8 meV. The LD and MD results were not affected by such a drastic truncation since the calculated distributions were extended down to zero frequency, although it

was also necessary to perform an extrapolation in E^2 in order to prevent spurious effects caused by statistical noise which become evident at low temperatures (below 1 K).

The $C_p(T)$ curves measured for both glass and polycrystalline samples are shown in figure 1, and a comparison between the calorimetric C_p curves and the neutron results at low temperatures is also shown. As can easily be seen, the curves measured by both techniques are rather close below 100 K for both the glass and crystalline cases. The glass transition is obvious at about $T = 105$ K which gives rise to a short-lived supercooled regime. The absence of such a transition in the crystal data is clearly apparent.

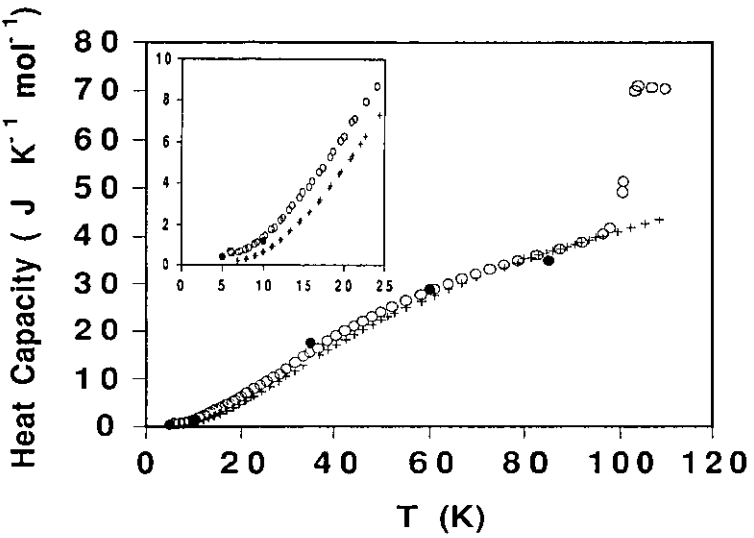

Figure 1. Constant-pressure heat capacities for polycrystalline (+) and glassy (O) samples. The full circles show the estimates for the heat capacity calculated from the frequency distributions measured by INS. The inset shows a comparison of the low-temperature region of these curves with the values calculated from the neutron scattering frequency distributions.

A comparison between the quantities calculated by means of LD and MD and those measured experimentally is shown in figure 2 as C/T^3 curves where data taken from [11] have also been included in order to compare the present measurements with previous data corresponding to a high-purity polycrystalline sample. As can clearly be seen upon inspection of figure 2(*b*), some small differences are seen between both sets of measurements especially at low temperatures, and on the other hand, rather noticeable discrepancies between the calorimetric curve and the one computed from the LD calculation appear below 10 K, where the predicted result lies substantially above the experimental one.

The low-temperature behaviour of the magnitudes corresponding to the glass is shown in figure 2(*a*), where the C/T^3 curves computed from the MD simulation are decomposed into rotational and centre-of-mass terms, the sum of these two contributions and the rotation–translation coupling terms respectively. Several

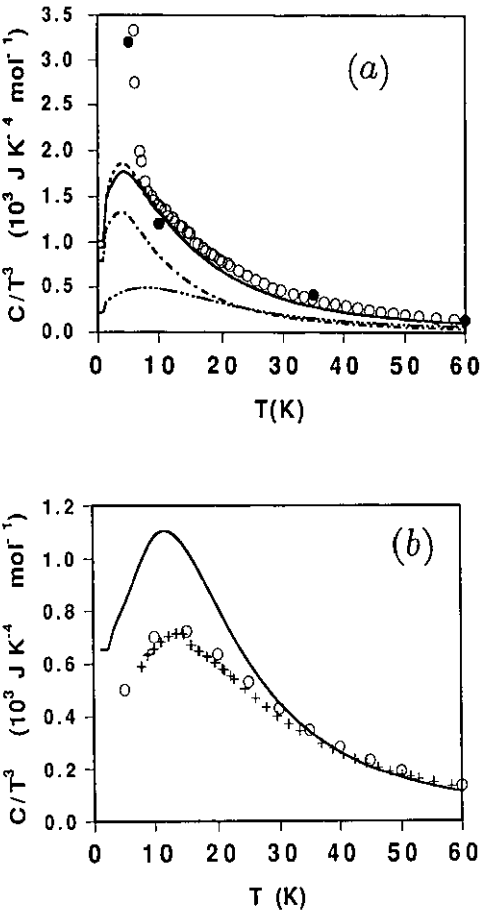

Figure 2. (*a*) Low-temperature region of the $C(T)/T^3$ curves for the glass sample. The data corresponding to the calorimetric measurement are shown by open circles, and the neutron results by full circles. The MD prediction is shown as a solid line, the rotational component by (— · · · —) line, the centre-of-mass by (— · —) and the sum of the latter two contributions by the dashed line on top of the solid line. The difference between the latter curve and the total MD prediction is due to the coupling terms. (*b*) A comparison between lattice dynamics (——) and the experimental (+) calorimetric result for the polycrystal. The open circles correspond to calorimetric data taken from [11].

comments are in order regarding this figure. First of all, from comparison of the present data with those taken from [11], it can be seen that an upper bound of temperatures up to where the Debye law is followed can be estimated to be about $T < 6$ K. A very approximate estimation of the value of the T^3 term contributing to the heat capacity can be made by means of fitting the data corresponding to the lowest temperatures using a T^3 law and gives a value of 0.50×10^{-3} J K^{-4} mol^{-1}. On the other hand, the glass shows, as expected, a strong deviation from the behaviour followed by the crystal as the temperature is decreased. From inspection of such a graph it can be seen that

(i) The maximum above the Debye value in the C/T^3 curve, which is visible

in the calorimetric measurements for the polycrystal, also appears in the LD result which shows a maximum centred at about 12 K. Such a departure from the idealized continuum behaviour should therefore be attributed to the purely harmonic part of the heat capacity, and in particular to the two intense peaks of mostly rotational character appearing at about 6 meV in the polycrystalline $g(E)$ (see below).

(ii) The rise in the heat capacity of the glass with decreasing temperature is also borne out by the MD results which show a pronounced maximum at about 3 K. Such a feature is clearly attributable to the centre-of-mass contribution to the specific heat, since the rotational and coupling terms show a far smoother behaviour in this temperature range [4].

(iii) A noticeable difference in the absolute values between the simulation and experimental results for the glass is clearly apparent below 8 K. Such a discrepancy can partly be accounted for if contributions not amenable to classical simulations (such as the one linear in T arising from tunnelling states which should become dominant below 1 K) are introduced heuristically.

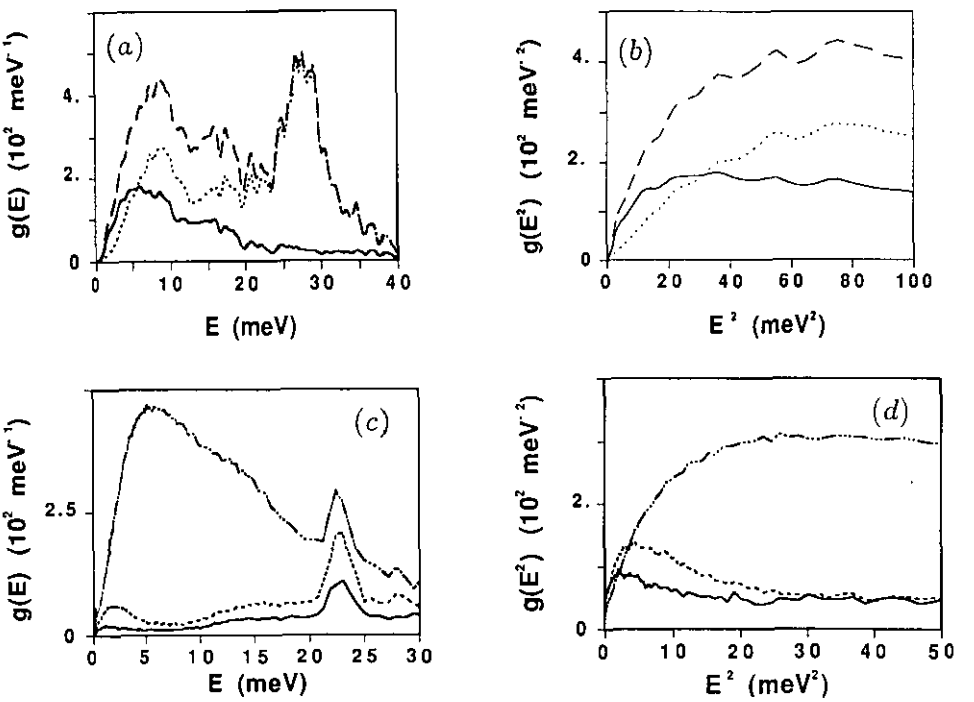

Figure 3. (*a*) The $g(E)$ calculated from the MD computer simulation corresponding to a thermodynamic state $T = 35$ K. The top line (– – –) represents the total (sum of rotational, centre-of-mass and coupling terms) function, the middle (·····) is the rotational contribution, and the lower (——) the purely centre-of-mass term. The total curve has been normalized to unit area. (*b*) The low-energy part of the components of the simulated $g(E)$ versus E^2. The same symbols as in figure 3(*a*) are used. (*c*)A comparison of the neutron $g(E)$ for $T = 35$ K (top), $T = 10$ K (middle) and $T = 5$ K (bottom). The curves have been normalized to $3k_BT$ to facilitate the comparison. (*d*) The low-energy parts of the distributions measured for $T = 35$ K, $T = 10$ K and $T = 5$ K versus E^2. The same symbols as in figure 3(*c*) are used.

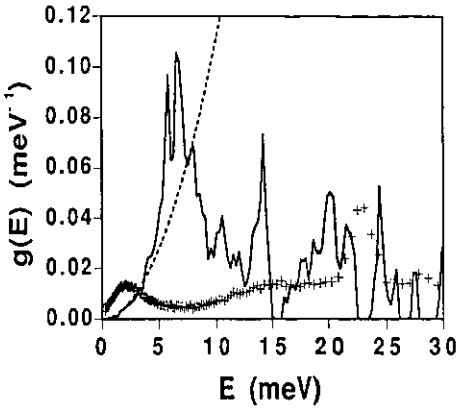

Figure 4. The solid line shows the $g(E)$ derived from the LD calculation for the crystal, the dashed line is a Debye curve drawn by means of fits of the low-energy region to a Debye law, and the crosses stand for the distribution for the glass at $T = 10$ K.

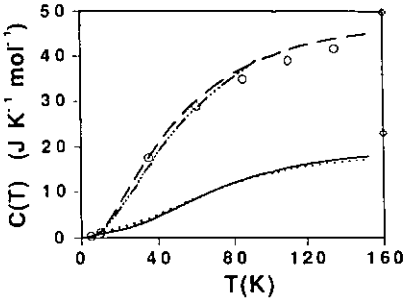

Figure 5. The solid and dashed lines show the calculated $C(T)$ using the INS $g(E)$ distributions measured at $T = 5$ K and $T = 10$ K. (— — —) represents the same quantity calculated using the distribution for $T = 35$ K. The open circles are the neutron data calculated using the distributions obtained for each temperature and the dash-dots line represent the calorimetric C_p.

(iv) Both $C_p(T)/T^3$ curves for the glass and crystal approach rather similar values for temperatures above 80 K up to the glass transition points which occurs at about 100 K.

The $g(E)$ functions of the computer MD simulations are shown in figure 3 as well as those corresponding to the lower temperature INS experiments. A comparison between the function arising from the LD calculations and the experimental INS data for the glass at $T = 10$ K is given in figure 4. The most salient features concerning these functions, for which some details can be seen in figure 3, and in particular the $g(E)$ versus E^2 curves are the following.

(i) All the curves show a low-frequency regime which can be represented by an E^2 term. A departure from this behaviour to another with higher exponents occurs at frequencies of about 1.5 meV, depending upon the temperature, and a further crossover through the Debye line also occurs at frequencies of about 6 meV, after which they show an increase substantially below the energy-squared behaviour. The experimental data from INS show a similar behaviour for temperatures of 35 K and above, although the overlap with the elastic line strongly complicates such a comparison.

(ii) In the glass phase at $T = 5$ K and $T = 10$ K a well resolved peak appears centred at about 2 meV. Such a feature disappears for $T = 35$ K and above, and the relative importance of the excess modes, taken as the difference between the observed and the calculated E^2 curves, decreases as the temperature is raised. A difference function, intermediate between the Debye law and the actual $g(E)$ measured by INS, was calculated. Due to the above-mentioned crossovers, it shows a pronounced peak located at about 4.2–5 meV, with temperature-dependent position and width.

(iii) The results for $g(E)$ from the MD simulation are able to reproduce the observed behaviour in a semiquantitative way for temperatures above 10 K. Below

this limit, the interparticle potential employed for the calculations seems to be too crude to account for all the observed features, especially those arising from mostly rotational motion, and is therefore are unable to reproduce the peak at 2 meV seen in the experiment.

(iv) From inspection of figure 4, it can be seen that the well resolved maximum in the glass $g(E)$ at the lowest achieved temperatures, is located within an energy region where the crystal follows an approximate E^2 law. Above 5 meV, and for the crystalline case, the intensity of the two mostly rotational peaks centred at about 6 meV, severely distorts such an idealized behaviour. A Debye $g(E)$, with the same area as the one calculated by LD can also be drawn. The calculated value for the Debye cutoff frequency is then of about 14 meV, located rather close to the intense peak at 14.6 meV which was shown to be characterized by sharp translational and rotational components [4].

Taking into consideration the above point, it seems clear that a rather complicated temperature dependence is expected for the glass heat capacity, even for relatively low temperatures (10–35 K). The term proportional to E^2 in the density of states will give rise to a contribution in T^3 at low temperatures which should be the dominant contribution between 1 K and 5 K (not reached in the present experiments), with a larger coefficient for the glass than for the polycrystal. In order to account for the complicated frequency-dependence observed in the $g(E)$ commented above, it becomes clear that fractional temperature exponents are required in order to account for these dependences. Such behaviour has been recognized in most of the glasses studied to date [12] and is therefore considered to be a universal characteristic of the vitreous state. For temperatures around and below 1 K a linear term from the contribution arising from tunnelling between two-level systems should be added but in the absence of measurements performed at these temperatures, and also due to the complicated temperature dependence exhibited by the C/T^3 curves, no further analysis was carried out regarding this topic.

A comparison between the $g(E)$ distributions derived from the INS measurements at $T = 5$ K, 10 K and 35 K is shown in figure 3(*c*). While some features are common to the three distributions, such as the relatively prominent peak at about 23 meV which arises from torsional oscillations (which will be discussed below), a shoulder at about 14 meV which can be related to the intense feature appearing in the LD calculation of figure 4, and the excess of modes at low frequencies, there are several distinctive features which appear below 35 K. First of all, the manifold of optical (mostly rotational) modes which show a maximum at about 6–7 meV in both the LD and MD results and which is also present in the experimental $g(E)$ at $T = 35$ K, has virtually disappeared at 10 K and below. This uncovers the well defined peak centred at about 2 meV which has been shown to be of harmonic nature [4] from the analysis of the temperature dependence of the inelastic intensies at such frequencies.

In order to shed some light on the drastic changes which occur between 10 K and 35 K, which are not associated with any clear calorimetric singularity, figure 5 shows a comparison of the $C(T)$ functions computed from the experimental $g(E)$ distributions for $T = 5$ K, 10 K and 35 K, with the corresponding theoretical values (i.e. every open circle corresponds, as in figure 1, to the value of the heat capacity calculated by integration of $g(E)$-weighted Einstein modes, at the temperature corresponding to each measurement), as well as with the $C_p(T)$ function from the calorimetric measurements. By inspection, it can be seen that the $g(E)$s measured

at $T = 5$ K and 10 K, basically contain the same dynamical information thus leading to a prediction for $C(T)$ with a high-temperature limit of about 23 J K^{-1} mol^{-1}, somewhat less than what could be expected for the case where the rotational motions were completely frozen. On the other hand, the curve computed using the $g(E)$ measured for $T = 35$ K contains all the relevant dynamics so that the prediction is reasonably close to both the $C_p(T)$ curve and the experimental points calculated at each temperature individually. The high-temperature limit of this curve also agrees with what is expected for a molecular solid of these characteristics.

In order to assess the predictive capability of the MD simulation, the estimated $C_v(T)$ curve is compared with the INS results in figure 6(*a*). As can be seen from the figure, the estimate of the contribution of internal molecular modes becomes relatively important at higher temperatures and, once added to the LD result, a fair agreement between calculation and experiment is achieved.

The low-temperature C/T^3 heat capacities calculated from the neutron $g(E)$ functions are finally compared with the one predicted from the MD simulation in figure 5(*b*). A strong anomaly is clearly seen as a very prominent peak centred at about $T = 0.5$ K in the curves obtained from the experimental densities of states, whereas the MD prediction peaks at about $T = 3$ K show a height one order of magnitude smaller than the experimental INS result.

Finally, the contribution due to the anharmonic effects of interparticle interactions (the anharmonic contributions arising from the methyl groups were taken into account previously) was estimated from $C_p(T) - C_v(T) - \alpha^2 VT/\chi_s(T)$, and some values for ΔC_v^{anh} have been obtained using the expansivity values referred to above for both glass and polycrystal cases. In the crystal, the estimate of the harmonic part of C_v was readily obtained from the curves resulting from the LD calculation, whereas the functions computed from the MD results were taken for the glass case. Such a procedure should substantially underestimate the ΔC_v^{anh} contribution for the glass since important anharmonic effects are built into the model potential used, and therefore only a lower limit of this magnitude can be given. The estimate for ΔC_v^{anh} for the crystal shows a quasi-linear temperature dependence, taking negligible values up to about 25 K and reaching a value of 5.4 J K^{-1} mol^{-1} at 80 K. The results for the glass show a more complicated dependence, showing a maximum at about 45 K with a value of 2.7 J K^{-1} mol^{-1}. The relevance of the temperature dependence of these magnitudes cannot be assessed due to the limitations already mentioned, but the order of magnitude for both phases can be favourably compared with a recent determination of this contribution for both polycrystalline and amorphous ice [13]. As a matter of fact, such large anharmonic contributions to the total heat capacity can be compared with results derived from a calculation performed by Leadbetter [14] some time ago for hexagonal ice, which in view of the recent INS results can be considered as a lower bound. Values as large as ten per cent of C_v were found in this calculation for temperatures near the melting point, where ΔC_v^{anh} exhibits a steep increase, and for temperatures about $T_m/2$ (i.e. comparable to 80 K for the methanol polycrystal), a lower bound of 0.6 J K^{-1} mol^{-1} was obtained. On the other hand the experimental datum at such temperatures, which was estimated from [13] amounts to 1.5 J K^{-1} mol^{-1}.

From computations of the Debye–Waller frequency integrals using the calculated LD and MD frequency distributions, values for the total mean-squared amplitudes of vibration of 0.0382 $Å^2$ for the polycrystal and 0.0375 $Å^2$ for the glass, using $g(E)$

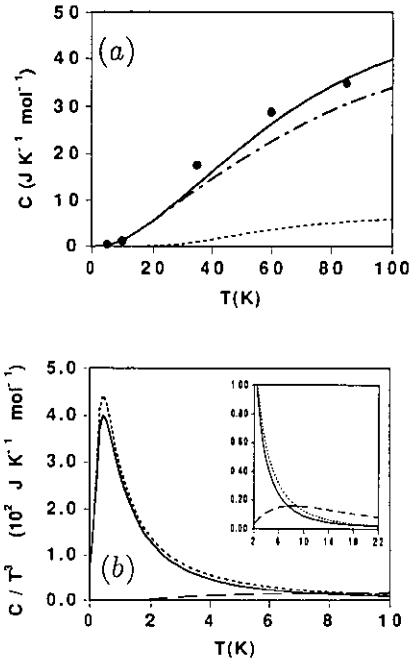

Figure 6. (*a*) A comparison between of the $C_v(T)$ calculated from the MD simulation (— · —), the contribution arising from internal modes (– – –), the total MD (including the internal modes) contribution, and the neutron data (●). (*b*) The anomaly in the low-temperature heat capacity as calculated from the neutron $g(E)$ distributions. The solid and dashed lines represent the quantities C/T^3 calculated using the distributions for T = 5 K and T = 10 K respectively. The inset shows a comparison with the MD prediction (— — —).

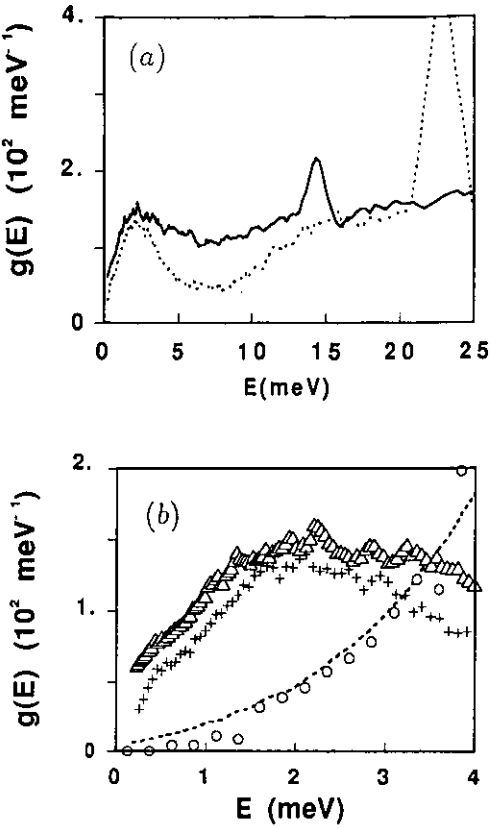

Figure 7. (*a*) A comparison of the $g(E)$ densities of states derived from INS on an incoherent (hydrogenated) sample (· · · · · ·) and a mostly coherent (deuterated) sample (——). Both curves, which have been calculated up to 50 meV, are normalized to unity. (*b*)A comparison of the $g(E)$ results for the polycrystalline sample (– – –), the LD results (○), the INS results for the incoherent sample (+) and the same quantity from the coherent counterpart (△). All the curves are normalized to unity and extend up to 50 meV.

corresponding to T = 10 K, were found. The interesting point to note is that the most important contribution to the total amplitude 0.0219 Å^2, comes from rotational movements, whereas the centre-of-mass motions only amount to 0.0148 Å^2, and the coupling terms account for the small difference between the total amplitude and the sum of rotational and translational contributions. Comparison of such values with those calculated for ice [14] at low temperatures or measured by INS at moderate ones [15], demonstrates the fact that the present results are substantially higher than those for H_2O ice where the total amplitude amounts to 0.0084 Å^2. The distribution of this amplitude between the translational and rotational components also differs since the former ones account for more than 97 per cent of the total atomic amplitude for

ice but only 38 per cent in methanol. On the other hand, the reported experimental neutron data which correspond to a temperature of 100 K, where anharmonic effects start to become noticeable, gives a value of 0.0272 Å^2 [15] for the proton motions, which can also be compared with the result of 0.030 Å^2 obtained from the Leadbetter calculation. A comparison with more recent results derived from high-resolution neutron diffraction from a single crystal of ice [16] gives an average value for the oxygen motion of 0.0086 Å^2, and a somewhat larger value for the average proton motion (0.015 Å^2) for $T = 15$ K, where the atomic motions can be considered purely harmonic in nature. Also, a diffraction study on the low temperature α-phase of methanol carried out at the same temperature [17], reported values for the vibrational amplitudes of the methanol protons within the range 0.0256–0.0330 Å^2 with an average value of 0.0297 Å^2, and values of 0.013 Å^2 and 0.0061 Å^2 for carbon and oxygen respectively. Such experimental findings confirm the substantially larger value of the mean-squared amplitudes of vibration in polycrystalline methanol, and consequently, it is expected that the ratio of zero-point to static-lattice energy will be, in the system under study, higher than that of normal ice. This may explain the large value found for the estimate of ΔC_v^{anh}.

4. Discussion and conclusions

The calorimetric results reported here can be compared with those measured some time ago [11, 18] covering temperature ranges of approximately 5–300 K and 20–110 K respectively. Both sets of data are in semiquantitative agreement in the range covered by both experiments, the maximum difference in absolute values between these two sets of experiments being less than 0.5 J K^{-1} mol^{-1} for the polycrystal and somewhat higher for the glass. The origin of such a discrepancy can be attributed to the small differences in sample composition between the two measurements [19].

The study reported here complements some previous findings [20, 21] where the collective excitations in this system were investigated by means of thermal [21] and cold [20] neutron spectroscopies using a mostly coherent-scattering (fully deuterated) sample. An analogous behaviour was noted when analysing the data for the coherent sample, and a comparison between the $g(E)$ for $T = 10$ K for both coherent and incoherent scattering samples is shown in figure 7(*a*). The main diferences between the two frequency distributions concern the intense peak at 23 meV in the incoherent sample which moves down to 14 meV in the coherent one. This can be assigned to torsional oscillations of the methyl group since a calculation with the potential barrier and moment of inertia given above predicts a frequency for the first excited state of 23.8 meV, and upon deuteration the frequency decreases to about 15 meV which can be accounted for after consideration of the different atomic masses involved. On the other hand, the existence of a well defined low-energy peak centred at about 2 meV is also borne out by the measurement using a coherent sample. This demonstrates the collective origin of these low-energy excitations, which are of a harmonic character [4].

A comparison of the low-frequency region (up to 4 meV) of the glass and crystalline $g(E)$ is finally shown in figure 7(*b*), where the $g(E)$ measured for a polycrystalline sample by INS and the corresponding LD results are also included. In such a frequency range both the experimental and LD results follow an E^2 curve quite closely, whereas a clear excess of vibrational modes is seen for both incoherent

and mostly coherent glass samples. The small difference in scale between the two curves is attributable to an incomplete averaging of the coherent effects since the maximum achievable momentum transfer was of about 2.5 $Å^{-1}$. The anomaly in the heat capacity displayed in figure 2(*a*) is therefore caused by this low-frequency feature since, once the temperature factors are introduced, only this low-energy part of $g(E)$ contributes significantly to the heat capacity.

The fact that the MD simulation, which uses a purely classical interparticle potential, is unable to account for the fine details of the dynamics below 10 K seems to indicate that, on the one hand, even at moderately low temperatures purely quantum phenomena such as tunnelling centres should be explicitly accounted for, and on the other hand one should always take care of the finite-size effects which may become difficult to tackle especially at rather low temperatures where long-wavelength thermal phonons are one of the dominant excitations. The existence of such tunnelling entities in this particular material will be explored in the future by means of dielectric-loss measurements

The short-range structure of the amorphous phase is known [10, 4] to be mostly composed of a tangled network of long winding chains formed by molecular units each bearing two hydrogen bonds. Apart from the excitations of acoustic origin, the lowest-lying modes of such a structure should be those characterized by small-amplitude oscillations around the H...O–H bonds, which should be able to couple to thermal phonons, and thus provide an efficient mechanism for the scattering of thermal phonons as well as an explanation of the origin of the observed anomaly in the specific heat. Such movements will have to be of a collective nature since the concerted motion of many units is required in order to preserve the structural integrity of the chains. A modelling of the interaction potential using *ab initio* results seems to be a prerequisite for a proper representation of the potential energy surfaces, since the interaction potential employed in the computer simulations [5, 22] is of a classical type (six mass points plus three centers of force) and only contains limited information regarding the fully anisotropic interactions between particles.

As a final conclusion, the present work has shown the presence of low-frequency excitations, peaked at about 2 meV, in a molecular glass which are the origin of the anomalous behaviour exhibited by the low-temperature heat capacity. The relevant movements appear to have much in common with the known phenomenology of long studied cases such as vitreous silica or the alkali-halide–alkali-cyanide glasses, in the sense that highly co-operative small-amplitude harmonic motions seem to be the common cause of the anomalies in the thermal behaviour of these chemically unrelated, amorphous materials.

Acknowledgments

This work has been supported in part by DGICYT grants No PB89-0037-C03 and MAT91-0923. The help given by Dr A J Dianoux of the Institut Laue–Langevin during the inelastic neutron scattering experiments is warmly acknowledged.

References

[1] Phillips W A 1987 *Rep. Prog. Phys.* **50** 1657

[2] Grannan E R, Randeria M and Sethna J P 1990 *Phys. Rev.* B **41** 7799
[3] Attempts to explain the temperature behaviour of the heat capacity in terms of mode-softening by strains or phonon scattering by localized modes are not borne out by experimental measurements. For a short review on this topic see
Buchenau U 1989 *Dynamics of Disordered Materials* ed D Richter *et al* (Berlin: Springer) p 172
[4] Bermejo F J, Alonso J, Criado A, Mompean F J, Martinez J L, Garcia-Hernandez M and Chahid A 1992 *Phys. Rev.* B **46** 6173
[5] Alonso J, Bermejo F J, Garcia-Hernandez M, Martinez J L, Criado A and Howells W S 1992 *J. Chem. Phys.* **96** 7696
[6] Davidson N 1962 *Statistical Mechanics* (New York: McGraw-Hill)
[7] Pitzer K S and Gwinn W D 1942 *J. Chem. Phys.* **10** 428
[8] Rudolph H, Avery J and Henningsen J O 1986 *J. Mol. Spectrosc.* **117** 38
[9] Stull D R, Westrum E F and Sinke G C 1969 *The Chemical Thermodynamics of Organic Compounds* (New York: Wiley)
[10] Marchi M and Klein M L 1989 *Z. Naturforsch.* a **44** 585
Sindzingre P and Klein M L 1992 *J. Chem. Phys.* **96** 4681
[11] Carlson H G and Westrum E F 1971 *J. Chem. Phys.* **54** 1464
[12] Nagel S R and Grest G S 1986 *Phys. Rev.* B **34** 8667
Pohl R O and Schwartz E T 1985 *J. Non-Cryst. Solids* **76** 117
[13] Klug D D, Whalley E, Svensson E C, Root J H and Sears V F 1991 *Phys. Rev.* B **44** 841
[14] Leadbetter A J 1965 *Proc. R. Soc.* A **287** 403
[15] Prask H J, Trevino S F, Gault J D and Logan K W 1972 *J. Chem. Phys.* **56** 3217. Data taken from table 3
[16] Values taken from
Kuhs W F and Lehmann M S 1987 *J. Physique Coll.* Suppl. 3 C 1 1–3
[17] Torrie B H, Weng S X and Powell B M 1989 *Mol. Phys.* **67** 575
[18] Sugisaki M, Suga H and Seki S 1968 *Bull. Chem. Soc. Japan* **41** 2586
[19] The previous work had used a dried sample, which leads to rapid crystallization proccess. The samples containing about 6% water show a far larger stability, remaining in the vitreous state for a few days if the temperature is kept below 50 K.
[20] Bermejo F J, Martinez J L, Garcia-Hernandez M, Martin D, Mompean F J, Alonso J and Howells W S 1991 *Europhys. Lett.* **15** 509
[21] Bermejo F J, Martinez J L and Garcia-Hernandez M 1990 *Phys. Lett.* **150A** 201
[22] Alonso J, Bermejo F J, Garcia-Hernandez M and Martinez J L 1991 *J. Mol. Struct.* **250** 147